Journal of Forests
2025 Vol. 12, No. 2, pp. 94-111
ISSN(e): 2409-3807
ISSN(p): 2413-8398
DOI: 10.18488/jof.v12i2.4408

Natural high forest cover dynamics in Aweta River watershed: A case of Southern Ethiopia

Wendafiraw Abdisa Gemmechis

School of Earth Sciences, College of Computational and Natural Science, Addis Ababa University, Ethiopia.
Email: wendeabdisaone@gmail.com

Article History
Received: 4 August 2025
Revised: 5 September 2025
Accepted: 9 September 2025
Published: 15 September 2025

Keywords
Awata River Watershed
Deforestation rate
Deforestation
GEE
Machine learning
Random forest.

ABSTRACT

Natural forest cover change for commercial and non-commercial purposes affects the forest itself and forest agents. The main aim of this study was to assess land cover change focusing on Anferara natural forest, located in the Awata River Watershed of Southern Ethiopia, over the past 38 years. Land use and land cover classification was performed using Google Earth Engine and utilized the random forest classifier. Landsat ^{TM} data for 1985 and 1994, Landsat $^{ETM+}$ for 2004, Landsat 8 (OLI) for 2014, and Sentinel-2 for 2023 were used. The overall accuracy assessments of all study years were greater than 96%. The results of the land use and land cover change classification reveal an increase in shrubland, which occupies large areas formerly covered by natural forest. This indicates that the arid and semi-arid land in Southern Ethiopia has expanded over time, primarily due to drought and anthropogenic barriers. Conversely, forest land decreased significantly from 433.8 square kilometers in 1985 to 79 square kilometers in 2023. Meanwhile, there was a notable increase in shrubland, agricultural land, settlement areas, and wetlands, from 3.18, 1.66, and 6.5 square kilometers in 1985 to 60.33, 98.4, and 38.78 square kilometers in 2023, respectively. The deforestation rate in the Awata River Watershed was approximately 67.58 square kilometers per year. Based on historical data and oral information, the deforestation in the area is primarily attributed to drought and other anthropogenic barriers.

Contribution/Originality: The study details how tropical high forests have been altered primarily due to commercial activities, especially for mining exploration. It also specifies the year when the forest cover experienced the most significant disturbance and identifies the land class predominantly classified as forest land.

1. INTRODUCTION

1.1. Background of the Study

A major contributor to global environmental change, land use/land cover (LULC) change has detrimental impacts on the structure and function of ecosystems. Additionally, it has a substantial impact on sustainable development and environmental quality [1, 2]. Historically, over the past millennium, LULC change has impeded sustainable development by impacting biological cycles, ecosystem services and functions, and climate [3]. Furthermore, changes in land use and land cover have been recognized worldwide as key factors of environmental change. They are also among the most difficult and persistent factors. Thus, managing the environment requires an understanding of the rate and processes of these changes [4, 5]. Likewise, changing information on LULC is the basis of global environmental stress research and regional governmental management. Also, automatic approaches are always required to update land maps for large-scale areas, and the techniques of change detection are the most important components of land-updating methods due to their significance as one of the serious world issues.[6]. Consequently, over the past 50 years there have been outstanding changes in the LULC pattern throughout the world

as a result of environmental degradation and the effects of climate change. Specifically, anthropogenic activities have caused a significant alteration of LULC change, especially in areas where population growth and climate change are severe [7, 8].

Furthermore, one of the most significant environmental issues facing the world is forest degradation, which actively affects biological cycles, ecosystem services and functions, and climate change. Amazingly, forests are vital global resources that influence a wide range of terrestrial functions affecting global health. It is an essential task to monitor their patterns and changes for efficient environmental resource management [9, 10]. According to Bera et al. [11], Forest cover or tree cover, as adopted from, is all vegetation taller than 5 meters in height. Forests are biological units with a vast social organization of living communities at work. Forests are a basic natural resource for living things; for example, they provide multiple ecosystem services ranging from local livelihoods and socioeconomic benefits to global ecological services [12]. In addition, forest communities are indispensable to preserving the world's balanced ecosystem. Since forests and forest communities are renewable resources and essential components of the entire environmental system [11, 13].

In contrast, because of a number of man-made and natural obstacles, forests are essential to the realization of a low-carbon green economy and sustainable development. Deforestation is a process that impacts both the forest domain and forest communities, and it is the reason why forest coverage is occasionally decreasing [14]. Similarly, deforestation is a terminology that is interchangeable with forest cover change. As such, deforestation is an environmental stressor that dramatically threatens biodiversity while having adverse, deep-rooted socioeconomic impacts [15]. Therefore, change in forest cover can affect both ecological and socio-economic systems [16]. On the other hand, forest transformation is defined as the changes occurring in a country's forest cover from a period of contraction to a period of expansion [17]. Yet despite forests' many values, forested land is being steadily converted to other uses, including cropland, pasture, mining, and urban areas, which can generate greater private economic returns [18]. Moreover, tropical forests are among the largest forest covers in the world, and tropical deforestation is one of the most significant drivers of biodiversity loss and carbon emissions [19].

Healthy forests are vital to sustainable growth and development. Therefore, understanding the trends, rates, and factors of forest cover change is important for various activities such as decision-making and management of this natural resource. To understand the dynamics of forest cover change caused by ecological and socio-economic factors, accurate and spatially explicit information is urgently required [16]. Forests contain more than 60,000 different tree species and provide habitats for a large majority of animal species. Approximately 1.6 billion people depend on forests for their livelihoods, including about 70 million indigenous people [20]. In 2020, 31% of the world's land area—4 billion hectares—was covered by forest, and of this total, about 45% was located in the tropical region. Since 1990, an estimated 420 million hectares of forest have been lost through deforestation. From 2015 to 2020, the rate of deforestation was estimated at 10 million hectares per year, though thanks to afforestation and reforestation in some regions, the net rate of deforestation was about half this [21]. African forests are increasingly in decline as a result of land-use conversion caused by human activities [22].

Particularly, Africa's forests are being depleted at a faster rate than those of any other continent. As a result of a major increase in the population growth rate that began after World War II, it is now running at an annual rate of 2.9 percent, resulting in massive demands for agricultural land, water, fuelwood, and other products [23]. Over the past two decades, Africa has experienced a rapid decline in its forest cover or tree cover [22]. Africa experienced a net loss of 4.0 million hectares per year, which is equivalent to 0.3% of the total African forest cover. This loss represented the second-largest net decrease in forests globally during the period. The continent's forests showed an average annual negative change rate of -0.62% from 2000 to 2005, making it one of the most affected regions in terms of forest decline [24]. Specially, as the climate in East Africa increasingly grows drier, the wet forest gradually disappears, and forests are becoming more and more common on the damp coastal hills, along the summits of mountains, and in strips that border rivers [22].

Historical sources indicate that an equivalent of 35% of Ethiopia's land area had once been covered by natural high forests [25]. According to Matthias [25], no reliable information on the extent and the location of the past and/or current forest cover existed for the country. The change detection analysis, based on satellite images from 1973 to 1976, indicates that in the seventies, natural high forests covered around 4.75% of the country. Around 10 to 15 years later, only about 2.20% of the country was still covered by undisturbed natural forests. On the other hand, according to Matthias, the annual deforestation rate was calculated at 163,600 hectares during the 1990s, and by the year 2000, remarkable forest stands could only be found in remote and/or inaccessible southern and southwestern parts of Ethiopia. Similarly, according to EFAP [26], it was stated that by the early 1950s, the forest cover of the country was reduced to 16% of the total area. By the early 1980s, this had decreased by 3.6%, and about 2.7% in 1989. The rate of deforestation is estimated at 150,000 hectares per year during the 1990s. This indicates that rapid deforestation and accelerated degradation of forest resources have led to the deterioration of the country's natural environment.

In 1974, Reider Persson wrote, in a ground-breaking survey of the world's forest resources, 'we know quite a lot about the moon, but we do not know how much of the earth is covered by forests and woodlands.' His words are still true. The problem is particularly acute for Africa [23]. Although we have the capacity to use remote sensing to monitor in considerable detail what is happening in tropical forests, no forest map has ever been produced for some countries, and for many, the statistics available from different sources are contradictory [23]. Additionally, remote sensing provides a defined process for gathering, integrating, and analyzing data within a geographic information system. Several classification methods, including supervised, unsupervised, and object-based image analysis, have been usefully applied by remote sensing satellites to map changes in forest cover within watersheds [27]. Remote sensing technologies provide a powerful tool for monitoring and managing forests on a large scale, offering the ability to detect changes in forest cover and health over time [10]. Nowadays, remote sensing-based technologies, such as Machine Learning (ML) and Deep Learning (DL) methods, are improving various problems seen in traditional classification methods for LULC. Several algorithms are essentially used for LULC classification, including Random Forests (RF), Artificial Neural Networks (ANN), and Support Vector Machines (SVM), which are some of the most powerful ML algorithms.

This study utilized Random Forest classifiers for the classification of LULC and analyzing the deforestation process in the Awata River Watershed from 1985 to 2023. Google Earth Engine, a cloud-based platform (https://earthengine.google.com/platform/) that is free for research and teaching purposes in geospatial analysis, was used to classify the data. It makes use of a JavaScript framework and offers a vast dataset, such as the Sentinel and Landsat archives.

The random forest can be defined as a versatile and smart machine learning method that can perform both classification and regression tasks. It can also perform dimensionality reduction methods, identify outlier values, treat missing data, and facilitate other steps of data exploration. It is an effective solution for most problems. It is known as an ensemble learning method, where a group of weak models are combined to form a powerful model. Random forests are simply a collection of decision trees generated using a random subset of data [28].

As a result, no studies have been conducted on the Jemjem plateau that focus on analyzing changes in forest cover, particularly in the Anferara forest. One of the well-known forests in southern Ethiopia is Anferara Forest, which is the highest forest in the nation. The Anferara forest in the Awata River Watershed was the focus of this project. It is a unique location because it is rich in mining sites, such as Adola and Shakiso, which are part of our country. This study investigates the trends of land use and land cover change, gains and losses of land use and land cover classes, and assesses the rates and positions of deforestation in the Awata River Watershed, focusing on Anferara forest over the past 38 years, from 1985 to 2023. The study concentrates on the natural high forest cover change in the Awata River Watershed (ARW) from 1985 to 2023. Changes in forest cover are among the main causes of forest degradation in southern Ethiopia, driven by high rates of anthropogenic activities. The increasing rate of

deterioration and change in forest resources is particularly noticeable in the research region, especially in the Anferara forest, and is causing growing concern. The study utilized Landsat TM data for 1985 and 1994, Landsat ETM+ for 2004, Landsat 8 (OLI) for 2014, and Sentinel-2 for 2023.

2. RESEARCH METHODS AND MATERIALS

2.1. Study Area Description

This study was conducted on the Awata River Watershed, located in Southern Ethiopia, which is a sub-part of the Adola and Shakiso mining areas, known for their mining activities. The total basin area is approximately 641.86 square kilometers. A significant portion of the study area lies within pastoralist regions. Consequently, much of the river basin is covered by shrubland, followed by Anferara Forest, which is part of the Jemjem Plateau. The upper river basin is predominantly covered by high forests, while the lower parts are characterized by shrublands, as it is situated in the lowland region of Southern Ethiopia. The Ghenale River basin is one of Ethiopia's larger highland basins, known as the Sidama Highlands, separated from the Bale Highlands by the Ghenale River valley, occupying the southwestern corner of this region. A notable feature is the Jemjem Plateau, an important coffee-growing area, and the Anferara Forest, which is a significant forest in this region and the focus of this study. The Awata River is a major tributary of the Ghenale River and is associated with one of the country's largest gold mining areas. The Awata River Watershed covers approximately 641.86 square kilometers. The upper basin is predominantly forested and used for agriculture, while the lower basin is covered by shrubland, grassland, and mining activities. The elevation of the basin ranges from 1,618 meters to 2,526 meters. The locational map of the Awata river watershed is illustrated in the Figure 1.

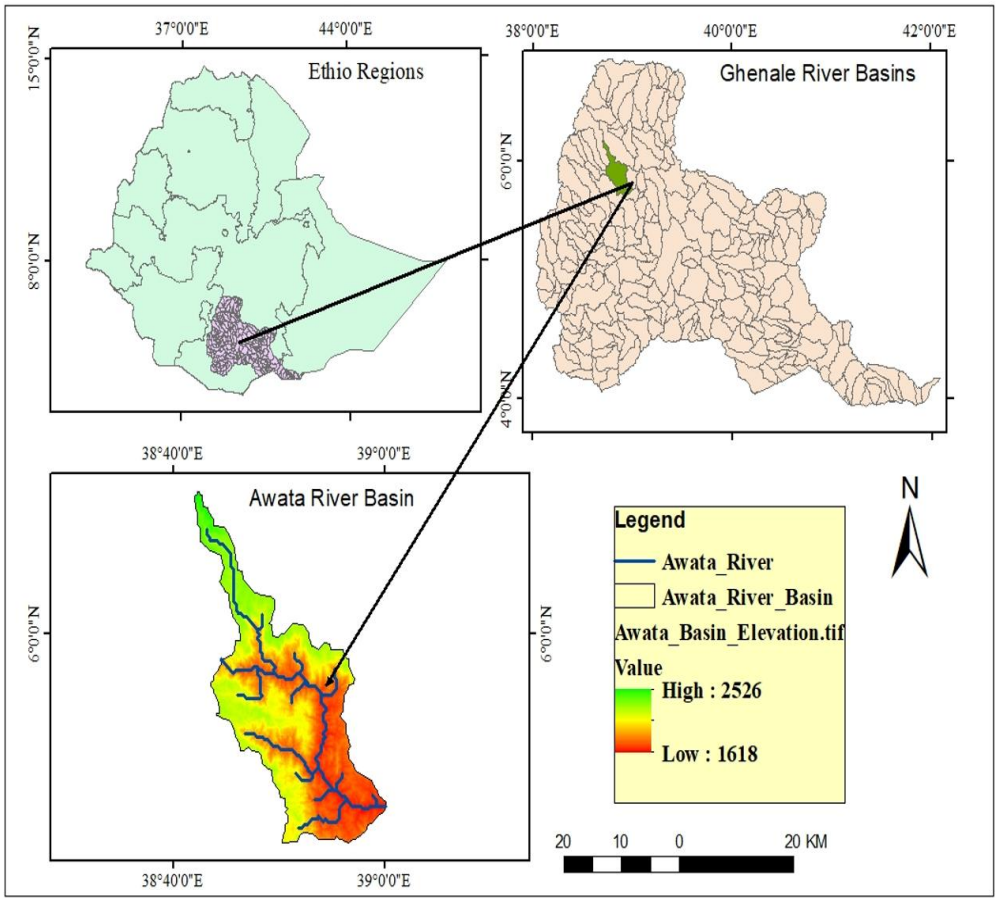

Figure 1. Locational map of study area.

2.2. Research Methodology and Methods of Data Collection

Forest cover monitoring based on geospatial data can significantly contribute to future forest management plans for reducing deforestation and implementing climate change mitigation policies [29]. Machine learning (ML) and deep learning (DL) based methods are current issues in technology used for various fields of study, especially for forest cover change analysis and prediction accuracy. The utilization of ML for vegetation identification through satellite imagery is a notable application. Typically, multispectral images captured by satellite sensors are employed as input parameters for the algorithms [10]. Random Forests are simply a collection of decision trees that have been generated using a random subset of data. The name "Random Forest" comes from combining the randomness used to select the subset of data with the presence of multiple decision trees, hence the term "forest" [30]. The random forest can be defined as a versatile and intelligent machine learning method that can perform both classification and regression tasks. It can also perform dimensionality reduction, identify outlier values, treat missing data, and facilitate other steps of data exploration. It is an effective solution for most problems. It is known as an ensemble learning method, where a group of weak models are combined to form a powerful model.

This project was conducted primarily using a quantitative research approach, employing random forest classifiers and other spatial analysis tools for further analysis. The Landsat series satellites (namely Landsat 1 to Landsat 9) are among the most commonly used and reliable imagery tools, providing one of the longest temporal records of space-based surface observations since 1972 [31]. For this study, Landsat ™ satellite data utilized for LULC classification of year 1985, and year 1994; Landsat $^{ETM+}$ utilized for LULC classification of year 2004; Landsat 8 captured by Operational Land Imager (OLI) utilized for the LULC classification of year 2014, and Santinel2 satellite was used for LULC classification of year 2023 Table 1. All classifications were performed using the Random Forest classifier algorithm in the Google Earth Engine platform.

Table 1. Specification of land use land cover change data collection methods.

Year	Data type	P/R	Date of Acq.	Resolution	Source
1985	Landsat ™		1983 Jan-May	60m	http://earthexplorer.usgs.gov/
1994	Landsat ™		1993 Jan-May	60m	http://earthexplorer.usgs.gov/
2004	Landsat $^{ETM+}$		2003 Jan-May	30m	http://earthexplorer.usgs.gov/
2014	Landsat 8		2013 Jan-May	15m	http://earthexplorer.usgs.gov/
2023	Santinel2b		2023 Jan-May	10m	https://scihub.copernicus.eu/

Land use land cover classification classes were selected based on the knowledge of the study area and the reality of the LULC classes that cover the study area. The selected land use land cover classes for the study and their descriptions are mentioned in the Table 2.

Table 2. Types of land use land cover classes and their descriptions.

No.	LULC classes	Their description
1	Agricultural land	It consists of all lands used for crop production and garden plantations.
2	Forest land	A continuous stand of trees at least 10 m tall, with their crowns interlocking.
3	Wetland	This land cover includes areas of mixtures of tall grass and water.
4	Grassland	Land covered with grasses and other herbs, either without woody plants or with woody plants not covering more than 10 per cent of the ground.
5	Shrub land	An open or closed stand of shrubs up to 2 m tall.
6	Settlement area	Includes residential areas like towns, villages, strip transportation, and commercial areas.
7	Mining area	It is surface mining that started the exploitation of different mining types.
8	Water body	It comprises rivers, streams, and small ponds.

2.3. Methods of Land use Land Cover Change Classification (Random Forest Classifier)

The basic principle of change detection through remote sensing is that changes in spectral signatures correspond with changes in land cover. The detailed procedure involves superimposing two period maps to identify the changes [32]. Moreover, the process of change detection is premised on the ability to measure temporal impacts [33]. It is

the process of identifying differences in the state of an object or phenomenon by observing it at different times (multi-temporal variations). On the other hand, change detection in remote sensing is defined as the process of identifying changes in the features of a scene through the joint analysis of a pair of images acquired at different times over the same geographical area [34]. Models are produced using machine learning processes to improve the accuracy of the results. Carefully choosing and taking into account the machine learning algorithms employed during the conceptual stages is essential to guarantee the creation of an efficient solution for any decision-making process [10].

The main aim of this study was detecting land use and land cover change over the past four decades, focusing on Anferara forest cover change. The classification process was performed using the Random Forest classifier algorithm on the Google Earth Engine (GEE) platform, which is free for research and academic purposes. GEE is a software used for geospatial analysis that utilizes a JavaScript scripting framework and offers access to extensive datasets, such as the Sentinel and Landsat archives. Land use and land cover change detection using a Random Forest classifier is an important technique for multispectral satellite data classification, aiding in understanding the optimal use of natural resources, conservation practices, and decision-making for sustainable development [35]. Random forest classification is an innovative machine-learning technique that utilizes multiple decision trees to classify data. It is an efficient and accurate way of classifying data, and it is widely used in many fields. Additionally, random forest classification is more robust to outliers than traditional parametric classification techniques [35]. Random forest algorithm are best for forest classification than others machine learning algorithms, according to Abigail et al. [36]; Joongbin et al. [37]; Lucian et al. [38]; Paul et al. [39]; Szilárd et al. [40] and Wan-Ni [41] the accuracy of the classification were ranges from 72% to 99% and they approved as random forest algorithm is best for forest classification. The detail work flow chart of the research methodology was illustrated in the Figure 2.

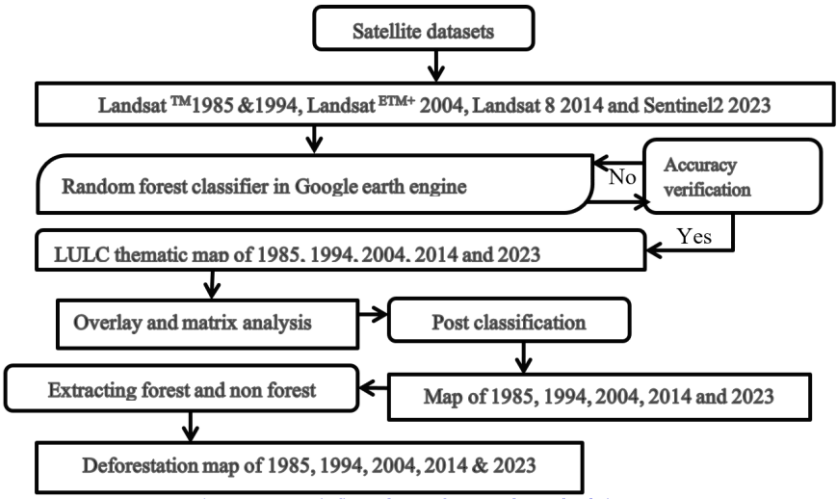

Figure 2. Work flow chart of research methodology.

Two images were interpreted using "-from, -to" information modifications. Cross-tabulation is used to compare classified images from two distinct data sets in order to ascertain the qualitative and quantitative features of changes for the following time periods: 1985–1994, 1994–2004, 2014–2023, and 1985–2023. A straightforward formula for expressing the amount and percentage of changes is as follows:

$$M = a - b \qquad (1)$$

$$P = \frac{(a-b)}{b} x100 \qquad (2)$$

Where (M) is the magnitude of changes, (P) is the percentage of changes, (a) is the first data, and (b) is the reference data [42].

2.4. Methods of Forest Cover Change Detection

Using multi-temporal data sets, change detection distinguishes regions where land use and land cover have changed between imaging dates [43]. Making decisions necessitates using data from spatial analyst are carrying out the required procedures [44]. The following eight principal land use/cover classes were recognized and categorized: agricultural land, forest land, wetland, grassland, shrubland, settlement area, mining area, and water body. Therefore, to create the deforestation map and forest area transition matrix for the periods 1985–1994, 1994–2004, 2004–2014, and 2014–2023, spatial analysis tools were employed for the study. The following formula was also used to determine the annual rate of deforestation (ARD) for the current study:

$$ARD(sq.km) = \frac{ay-by}{t} \quad (3)$$

Where ARD is the annual rate of deforestation in hectares, ay is the recent year forest cover in square kilometers, by is the initial year forest cover in square kilometers, and t is the number of years between ay and by.

3. RESULT AND DISCUSSION

3.1. Accuracy Assessment of Land Use Land Cover Classification

Landsat TM for the year 1985 and 1994, Landsat ETM+ for the year 2004, Landsat 8 (OLI) for the year 2014, and Sentinel-2 for the year 2023 were utilized for the LULC change classifications of the Awata River Basin. The Google Earth Engine platform was used to classify LULC. In essence, the number of correctly categorized ground truth pixels represents the classification accuracy. Maps usually contain inaccuracies; therefore, we must consider their accuracy as well as whether it is adequate for the purposes for which the study intends to use the data. Based on the average of the accuracies for each class on the map, the accuracy assessment's outcome provides the map's overall accuracy. Since accuracy evaluation restricts the classification findings of remotely sensed imaging data, it should be processed once the categorized image is incorporated into additional analysis. To do this, an error matrix must be used to evaluate a categorized map's accuracy and compare it with referenced data. The original classified images and Google Earth images from the years 1985, 1994, 2004, 2014, and 2023 were utilized to evaluate the classifications' correctness (Figure 3).

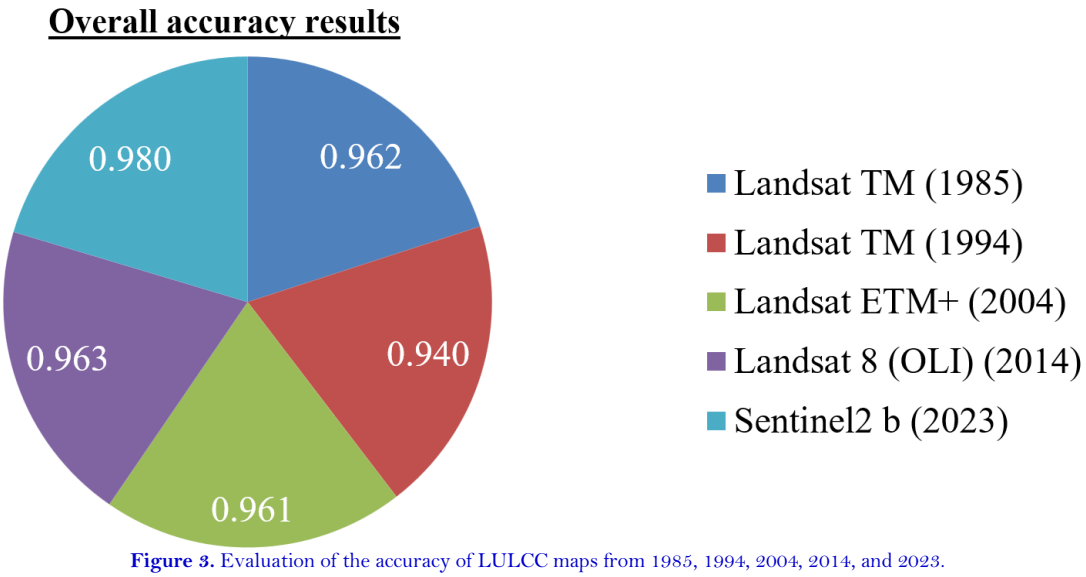

Figure 3. Evaluation of the accuracy of LULCC maps from 1985, 1994, 2004, 2014, and 2023.

Figure 3 portray the classification accuracy for each study year. The results of Sentinel2 2023 classification accuracy show that the highest recorded overall accuracy (0.980) and the rest of the overall accuracies (0.963, 0.961, 0.940, and 0.962) were for the years 2014, 2004, 1994, and 1984, respectively.

3.2. Land Use Land Cover Changes Analysis

The land use and land cover change was analyzed for the years 1985, 1994, 2004, 2014, and 2023. Table 3 lists the coverage areas for each LULC class for every study year. The results indicate that forest land was the only class that decreased from the initial to the final year, according to the LULC categorization statistics. In 1985, forest land occupied 433.8 square kilometers, but by 2023, it had dropped to 79 square kilometers. Conversely, the largest class increased was shrub land, which expanded to 339.1 square kilometers in 2023 after covering 120 square kilometers in 1985, with the addition of the highest lands. Between study years, the remaining land classes agricultural land, wetland, grassland, and settlement area periodically increased Table 3.

Table 3. Land use land cover change coverage in kilometer square and percent for all study years.

No.	LULC type	LULC coverage in percent and square kilometer									
		2023	%	2014	%	2004	%	1994	%	1985	%
1	Agricultural land	60.33	9.40	20.52	3.20	20.89	3.25	3.4	0.53	3.18	0.50
2	Forest land	79	12.31	217.45	33.88	242.45	37.77	349.4	54.44	433.8	67.58
3	Wetland	38.78	6.04	37.1	5.78	36.8	5.73	1.7	0.26	6.5	1.01
4	Grassland	16.7	2.60	12.6	1.96	13	2.03	5.44	0.85	9.15	1.43
5	Shrub land	339.1	52.83	319.7	49.81	252	39.26	216.387	33.71	120	18.70
6	Settlement area	98.4	15.33	21.25	3.31	13	2.03	1.34	0.21	1.66	0.26
7	Mining area	3.32	0.52	4.86	0.76	2.72	0.42	0.193	0.03	0	0.00
8	Water body	6.23	0.97	8.38	1.31	61	9.50	64	9.97	67.57	10.53
Total		641.86	641.86	100.00	641.86	100.00	641.86	100.00	641.86	100.00	641.86

The two areas of classes where LULC changed were mostly visible were forest land and shrub land, with negative and positive change respectively. During the study period, forest land decreased from 67.6% in the year 1985 to 12.3% in the year 2023, while shrub land increased from 18.7% in the year 1985 to 52.8% in the year 2023 Table 3.

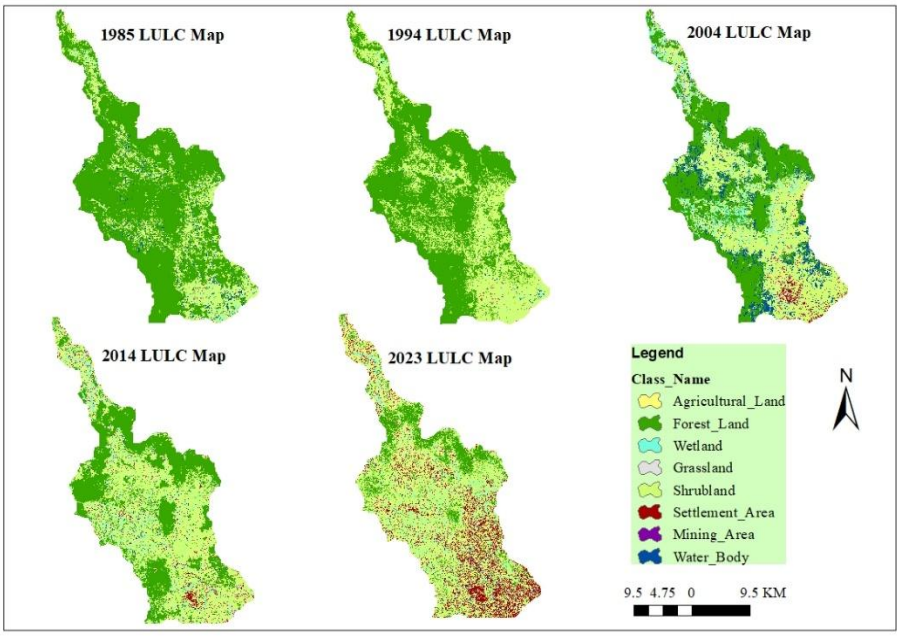

Figure 4. Classified LULC map of Awata River Watershed in 1985, 1994, 2004, 2014, and 2023.

The remaining land classes agricultural land, wetlands, grasslands, settlement areas, and mining areas have increased somewhat during the study periods, while the water body's coverage has decreased from 10.5% in 1985 to 1% in 2023; it is the only land type in the study area to lose coverage next to forest land. Since the goal of the study was to examine the Anferara forest, the LULC map for all study years was shown in Figure 4. The map showed that the majority of the forest land had been converted to agricultural land and shrubland, primarily as a result of the growth of grazing and agricultural expansion.

As seen in Figure 4, the shift in forest land around rivers was directly related to the local population's practical way of life. The region is linked to pastoralist and mining exploratory groups; the majority of the mining sites are situated along riverbanks, and grazing is also spread out along riverbanks. As a result, deforestation was established there rather than elsewhere in the study area. The main portions of the basin are covered by forest land in the first year of the study, although there were no areas designated for mining exploration in the initial year of 1985. Nonetheless, there are minor tracts of agricultural land and settlement areas because the majority of the local population's economic activity is pastoralist, which allowed the grazing land to turn into arable land and commercial areas (mine and settlement). Agriculture land, forest land, wetland, grassland, shrub land, settlement area, mining area, and water body covered 3.18, 433.8, 6.5, 9.15, 120, 1.66, 0, and 67.57 square kilometers of land during the first research year Table 3. According to the 1985 classified LULC results, forest land accounted for one-third of the study area, or 433.8 square kilometers, whereas agricultural land accounted for only 3.18 square kilometers, and there was no mining area.

Wetland, grassland, shrub land, mining area, settlement area, agricultural land, forest land, and water body shares in 1994 were 3.4, 349.4, 1.7, 5.44, 216.387, 1.34, 0.19, and 64 square kilometers, respectively (Table 3). In 2004, the classification map shows that the amount of forest land surrounding the expanding settlement areas has decreased, while the number of settlement areas has increased and encompasses a sizable portion of the basin's middle and southern regions. During 2004, the shares of agricultural land, forest land, wetland, grassland, shrub land, settlement area, mining area, and water body were 20.89, 242.45, 36.8, 13, 252, 13, 2.72, and 61 square kilometers, respectively. Over the fourteen-year period, forest land and water bodies decreased by 191.35 and 6.57 square kilometers, respectively, whereas settlement areas and agricultural land increased by 11.34 and 17.71 square kilometers, respectively Table 3.

Furthermore, the 2014 land use and land cover map shows that the study area's forest land is drastically decreasing while shrub land is growing. Agricultural land, forest land, wetland, grassland, shrub land, settlement area, mining area, and water body shares are 20.52, 217.45, 37.1, 12.6, 319.7, 21.25, 4.86, and 8.38 square kilometers respectively in the year 2014 Table 3. This research year, in contrast to previous years, saw a little decline in grassland and agricultural land.

Finally, the 2023-year LULC map shows an incredible loss in forest land, with the forest cover diminishing from 433.8 square kilometers in 1985 to 79 square kilometers in the last year. The decline of mining sites in 2023 is a result of policy changes in the study area. It decreased from 4.86 square kilometers in 2014 to 3.32 square kilometers in 2023. Wetland, grassland, shrubland, forest land, settlement area, mining area, and water body share 60.33, 79, 38.78, 16.7, 339.1, 98.4, 3.32, and 6.23 square kilometers, respectively, in 2023, as shown in Table 3. In general, the Awata River basin experienced a sharp decrease in water bodies and forest areas over the course of 38 years, while shrubland, agricultural lands, settlement areas, and mining areas increased significantly.

3.3. Loss And Gain of Land Use Land Cover Change

An estimated 87 percent of Ethiopia's highlands were covered by forests and woodlands in the past, but by 1950, this had dropped to 40 percent. Additionally, historical sources show that in the 1970s and 1980s, natural high forests covered an area equivalent to 35 percent of Ethiopia's geographical area [25, 45]. Similarly, in 1985, two-thirds of the Awata River basin was covered by forest, but over time, this area has unexpectedly decreased. The increment or

reduction in land use and land cover classes between the study years is referred to as gain and loss. Thus, using the gains and losses formula in square kilometers, the land use land cover change analysis was tested for all land classes for the research periods of 1985-1994, 1994-2004, 2004-2014, and 2014-2023 Table 4.

Table 4. Land use land cover change (sq. km) as well as losses and gains of LULC classes (sq. km).

No.	LULC type	Classification year					Gain & Loss (sq. km)				
		1985	1994	2004	2014	2023	1985-1994	1994-2004	2004-2014	2014-2023	1985-2023
1	Agricultural land	3.18	3.4	20.89	20.52	60.33	0.22	17.49	-0.37	39.81	57.15
2	Forest land	433.8	349.4	242.45	217.45	79	-84.4	-106.95	-25	-138.45	-354.8
3	Wetland	6.5	1.7	36.8	37.1	38.78	-4.8	35.1	0.3	1.68	32.28
4	Grassland	9.15	5.44	13	12.6	16.7	-3.71	7.56	-0.4	4.1	7.55
5	Shrub land	120	216.387	252	319.7	339.1	96.387	35.613	67.7	19.4	219.1
6	Settlement area	1.66	1.34	13	21.25	98.4	-0.32	11.66	8.25	77.15	96.74
7	Mining area	0	0.193	2.72	4.86	3.32	0.193	2.527	2.14	-1.54	3.32
8	Water body	67.57	64	61	8.38	6.23	-3.57	-3	-52.6	-2.15	-61.34
Total		641.86	641.86	641.86	641.86	641.86	641.86				

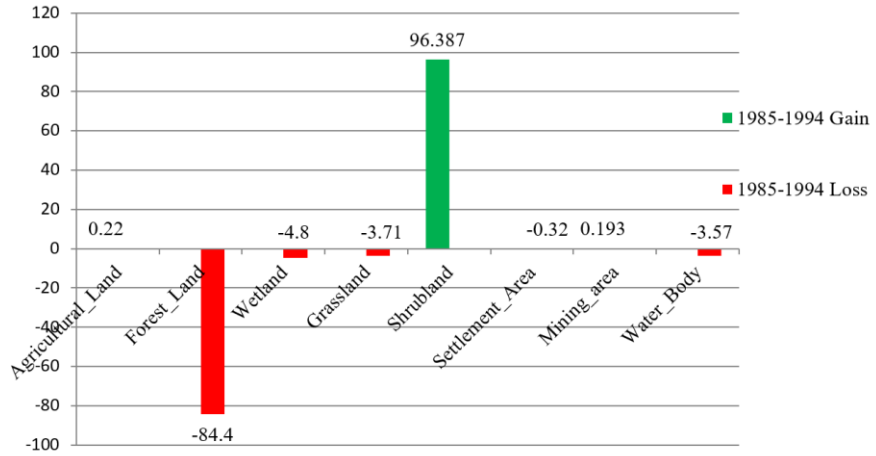

Figure 5. Gain and loss of LULC change between 1985 & 1994 in sq. km.

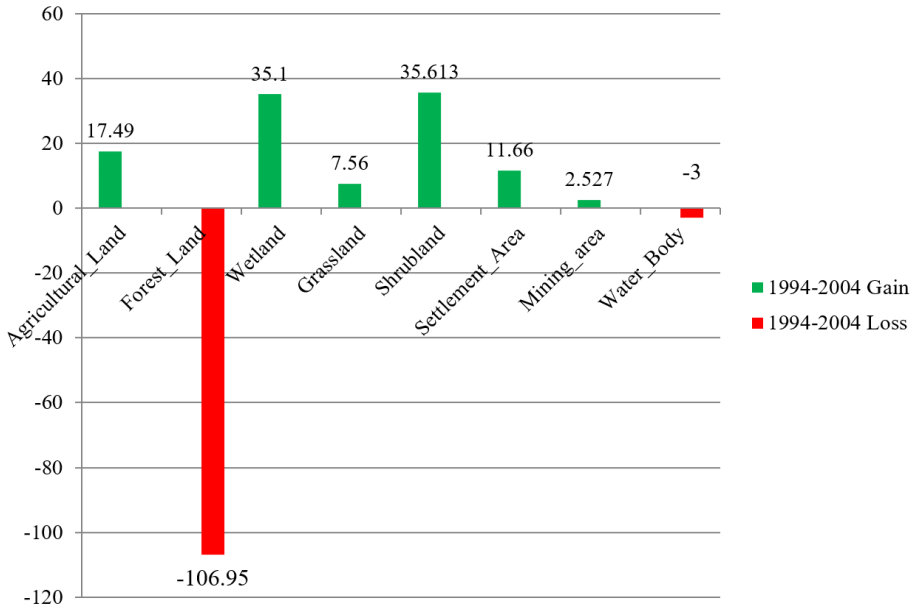

Figure 6. Gain and loss of LULC change between 1994 & 2004 sq. km.

According to the land use land cover change losses and gains, forest land was the class that lost the most area compared to the other LULC classes, losing 84.4 square kilometers. In contrast, agricultural land, settlement area, and mining area gained 0.22, 0.32, and 0.193 square kilometers over the same ten-year period, while shrubland gained 96.387 square kilometers. Over a ten-year period, wetland, grassland, and aquatic bodies lost 4.8, 3.71, and 3.57 square kilometers, respectively Figure 5.

Figure 6 shows the change in land use and land cover between 1994 and 2004. It shows that, out of the other classifications, forest land and water bodies have lost the most, with the forest land losing 106.95 square kilometers and the water bodies losing 3 square kilometers during this time. On the other hand, between 1994 and 2004, the following classifications of land saw increases: agricultural land, wetland, grassland, shrub land, settlement area, and mining area. These areas gained 17.49, 35.1, 7.56, 35.613, 11.66, and 2.527 square kilometers, respectively, Figure 6.

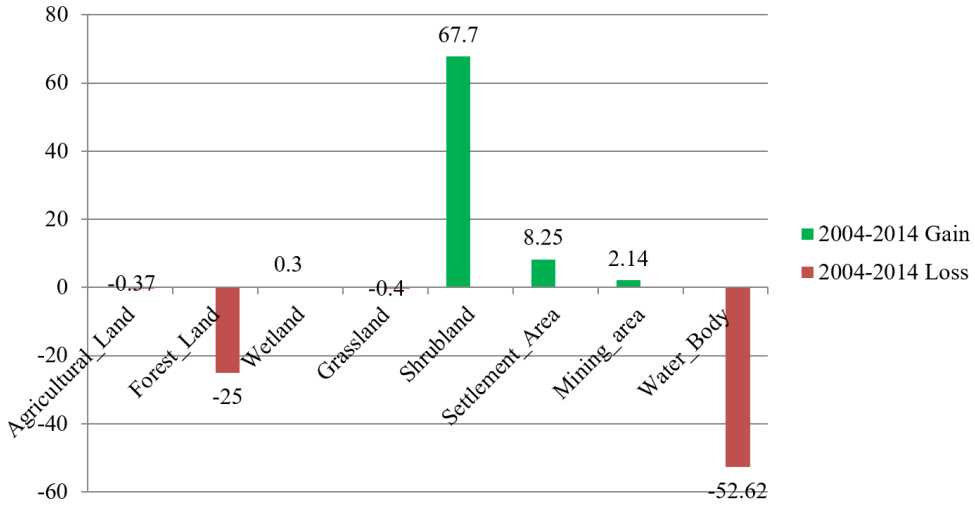

Figure 7. Gain and loss of LULC change between 2004 & 2014 sq. km.

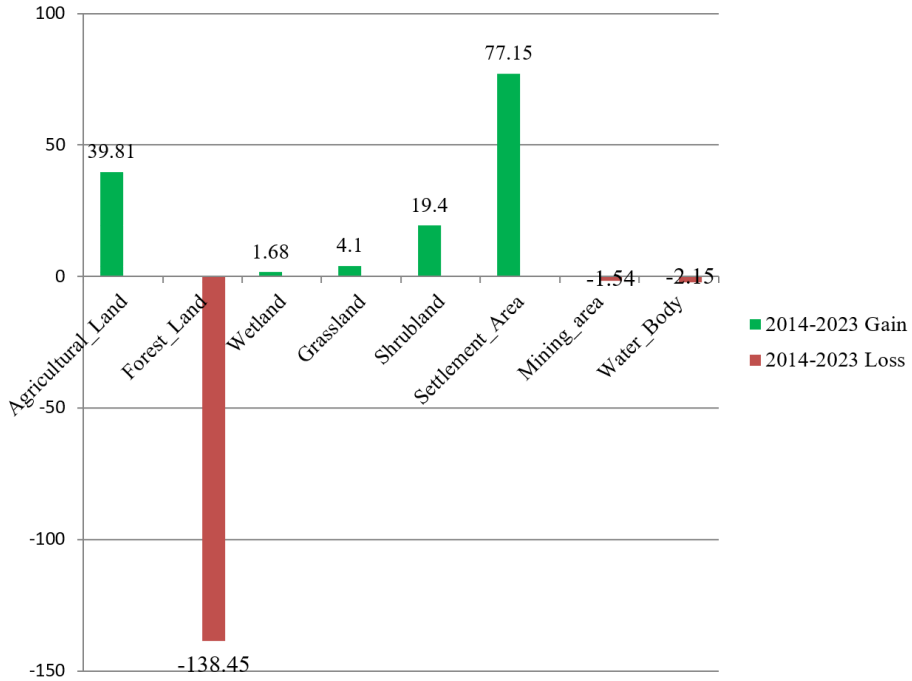

Figure 8. Gain and loss of LULC Change between 2014 & 2023 sq. km.

In addition, the loss and gain of land use land cover change are analyzed for land use land cover change classification of 2004-2014 and 2014-2023 study years. According to the analysis of gains and losses of LULC between 2004- and 2014-years, shrub land, settlement area, and mining area were land classes that gained land between these

study periods. Shrub land gained 67.7 square kilometers, settlement areas gained 8.25 square kilometers, and mining areas gained 2.14 square kilometers. On the other hand, agricultural land, forest land, wetland, grassland, and water body land classes were the classes of land that lost land between these study periods. They lost 0.37, 25, 0.3, 0.4, and 52.62 square kilometers, respectively. Shrub land was the class that gained the highest square kilometers in this study period, while water bodies were the classes that lost the highest square kilometers in this study period Figure 7.

The other study periods analyzed were between 2014 and 2023. According to the gain and loss of LULC during these periods, forest land, mining areas, and water bodies were the classes that experienced loss, with reductions of 138.45, 1.54, and 2.15 square kilometers, respectively. The remaining classes agricultural land, wetlands, grasslands, shrublands, and settlement areas gained in this period, increasing by 39.81, 1.68, 4.1, 19.4, and 77.15 square kilometers, respectively, to their former coverage Figure 8.

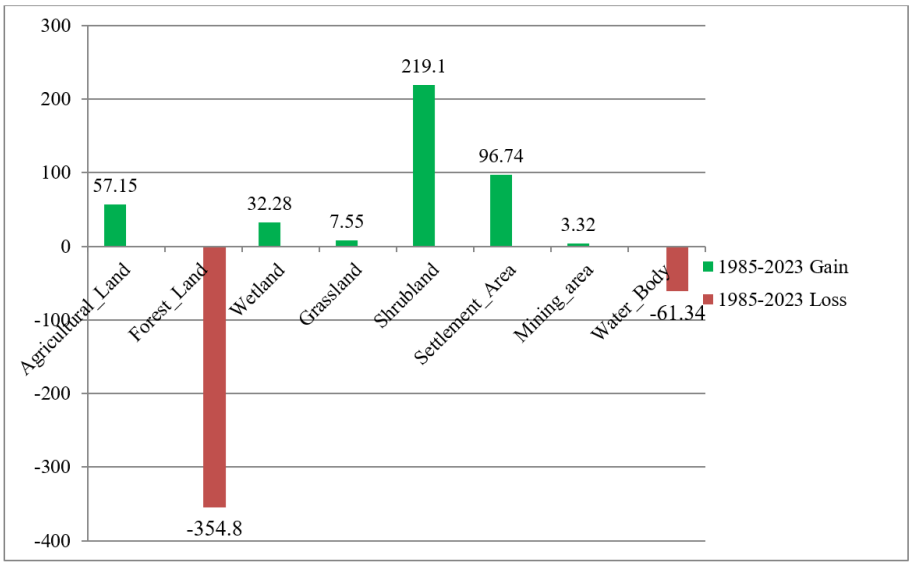

Figure 9. Gain and Loss of LULC Change between 1985 & 2023 sq. km.

In general, between 1985 and 2023, forest land is the dominant land cover that lost more area than the others; it lost 354.8 square kilometers. Meanwhile, shrub land was the dominant land cover that gained the highest land area among all study years; it gained 219.1 square kilometers between 1985 and 2023. This was followed by settlement area and agricultural land, which gained 96.74 and 57.15 square kilometers, respectively Figure 9.

3.4. Forest Cover Change Detection Analysis

In Africa, subsistence agriculture remains a key driver of forest loss, yet commercial agriculture tends to expand over time, accompanied by small-scale timber extraction for energy, though this is mainly associated with forest degradation rather than deforestation [46]. According to Matthias [25], the change detection analysis, based on satellite images from 1973 to 1976, indicates that in the seventies, natural high forests covered around 4.75% of Ethiopia. Around 10 to 15 years later, only about 0.20% of the country was still covered by undisturbed natural forests, and the annual deforestation rate was calculated at 163,600 hectares. Today, remarkable forest stands can only be found in remote and/or inaccessible southern and southwestern parts of the country. This study was conducted in the southern part of Ethiopia, specifically focusing on Anferara Forest, which is part of the natural high forests of the Jemjem Plateau.

In the Awata River Watershed, small-scale timber extraction and subsistence agriculture are key factors contributing to deforestation.

3.4.1. Rate and Frontiers of Deforestation in the Study Area

The conversion of forested areas to non-forest land was a series of problems in the study area. The Awata River watershed deforestation rate was determined for periods between 1985 & 1994, 1994 & 2004, 2004 & 2014, 2014 & 2023, and 1985 & 2023 Table 5.

Table 5. Annual rate of deforestation in the Awata River watershed for all study years in square kilometers.

LULC type	Forest cover in (sq. km)					Annual rate of deforestation (sq. km)				
Forest_land	2023	2014	2004	1994	1985	1985-1994	1994-2004	2004-2014	2014-2023	1985-2023
	79	217.45	242.5	349.4	433.8	301.20	207.51	193.21	54.84	67.58

The Awata River watershed deforestation rate results indicate that between 1985 and 1994, 301.20 square kilometers of forest were cleared; this deforestation rate is the highest when compared with other study periods. Additionally, the annual deforestation rates for the periods between 1994 and 2004, 2004 and 2014, and 2014 and 2023 are 207.51 (sq. km)/year, 193.21 (sq. km)/year, and 54.84 (sq. km)/year, respectively. The overall rate of deforestation in the Awata River watershed over 38 years was 67.58 square kilometers per year Table 5. Awata River watershed's annual rate of deforestation was high during the initial study years, specifically between 1985 and 1994. It was described as a period of high transition from grazing land to arable land in the study area Figure 10.

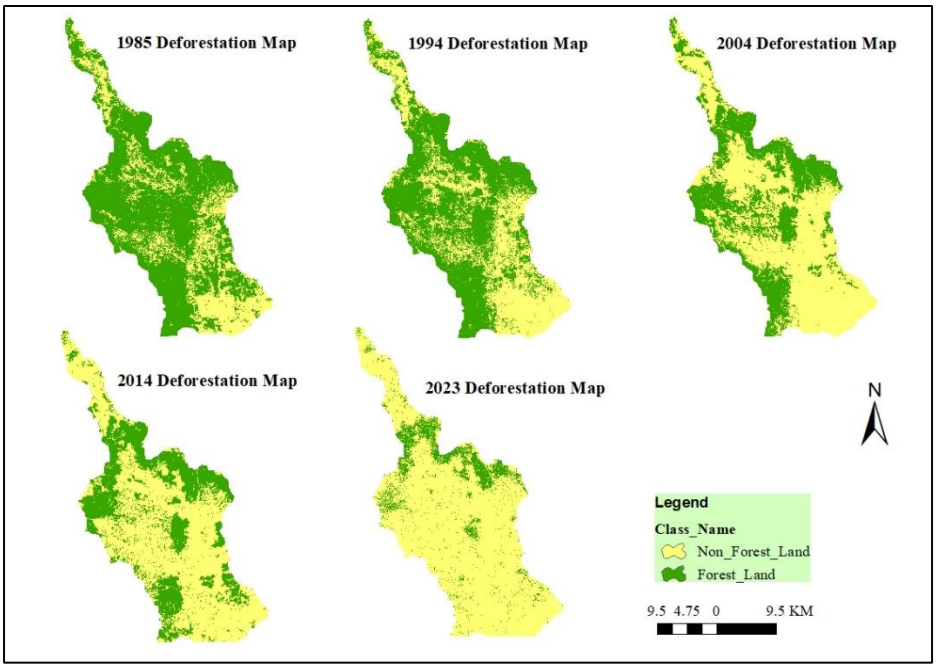

Figure 10. Deforestation map of Awata River watershed in 1985, 1994, 2004, 2014 and 2023 years.

The results of the annual deforestation rate indicate that the overall study period from 1985 to 2023 had an average of 65.78 square kilometers of deforestation per year. According to the standard level of deforestation rate classified by FAO, this falls under the high deforestation rate [46]. Deforestation pattern maps are shown in Figure 10. The results indicate that deforestation or forest transitions to other LULC are more prominent around the rivers. In 1994, the deforestation areas are located in the northern portion of the basin, the southern part of the basin, and the southeastern portion of the ARB. Similarly, the deforestation locations in 2004 are found in the southern, eastern, central, and western parts of the basin. During this period, the deforestation area was the highest relative to other transition periods. Conversely, in 2014 and 2023, the high forest areas of the basin are cleared in all locations, especially in areas favorable for agricultural activities and grazing. Finally, the natural forest persists only in the steepest parts of the basin and around complex landscapes of the Anferara, as shown in Figure 10.

3.4.2. Conversion of Forest Land to Non-Forest

In the study area, natural forests were being transformed into different land uses at an alarming rate. Figure 11 shows data regarding the conversion of forests to other land uses and land covers. Large tracts of forest land were converted to shrub land in all research years, according to the conversion of forest land to specific land use and land cover. These areas totaled 98.704, 80.008, 62.120, and 123.628 square kilometers, respectively, in 1985–1994, 1994–2004, 2004–2014, and 2014–2023. High tracts of forest land were turned into settlement areas between 2014 and 2023, while sizable tracts of forest land were converted into wetlands between 1994 and 2004 and 2014 and 2023. The total area of the converted forest land was 15.828 square kilometers and 7.150 square kilometers, respectively.

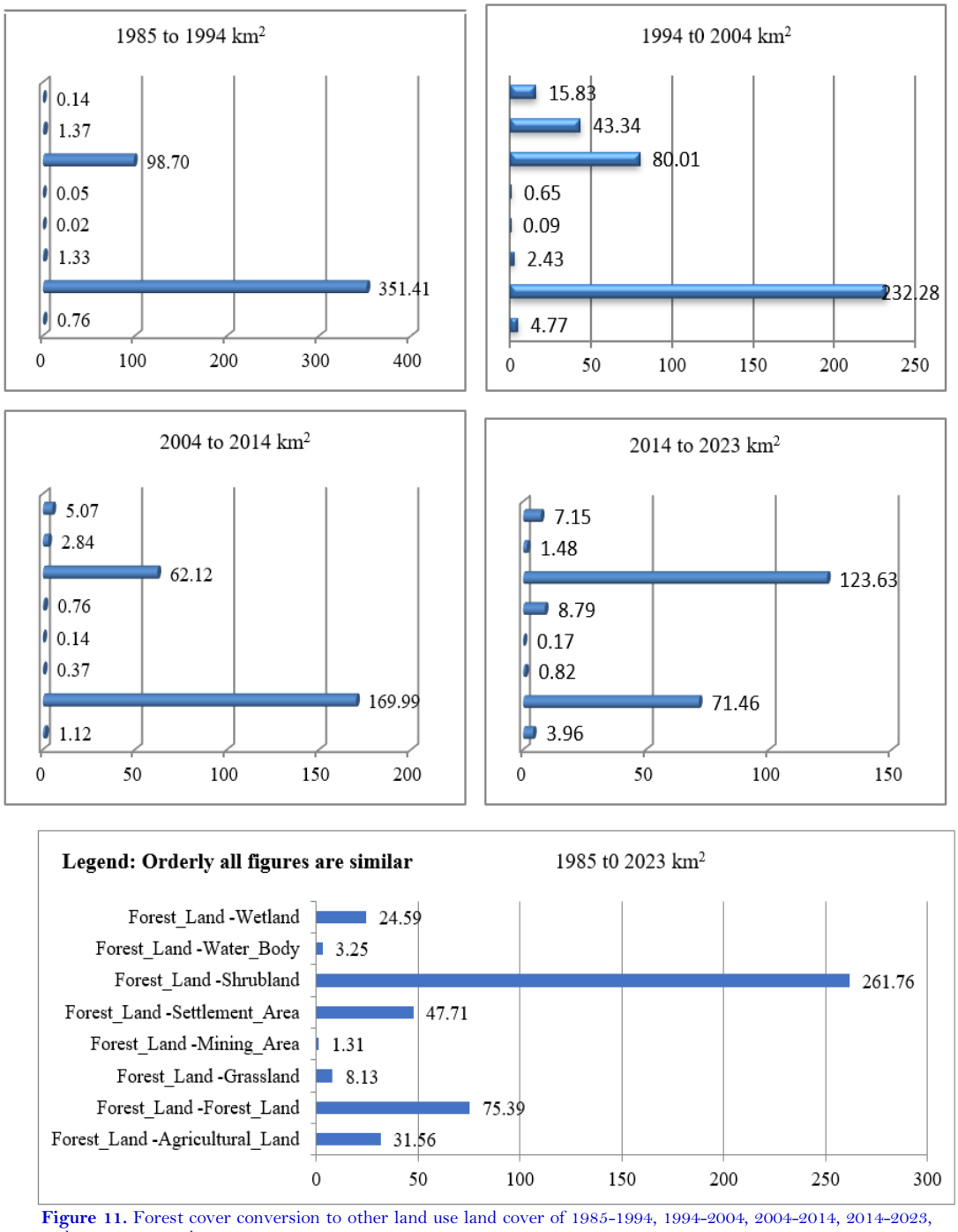

Figure 11. Forest cover conversion to other land use land cover of 1985-1994, 1994-2004, 2004-2014, 2014-2023, and 1985-2023 study years.

In addition, the largest area relative to the other eras under study, 43.345 square kilometers, was converted into aquatic bodies between 1994 and 2004. The conversion of forest land to mining regions is an intriguing development. During the years 2004–2014 and 2014–2023, the highest percentage of forest land was converted to mining areas; the corresponding areas were 0.138 and 0.167 square kilometers. During the research periods 1985–1994, 1994–2004, 2004–2014, and 2014–2023, the remaining land areas were 351.406, 232.278, 169.990, and 71.458 square kilometers, respectively Figure 11.

Commonly, between 1985 and 2023, 24.590 square kilometers of forest land were converted to wetland, 3.248 square kilometers to water bodies, 261.757 square kilometers to shrub land, and 47.714, 1.311, 8.126, and 31.564 square kilometers to mining, settlement, grassland, and agricultural land, respectively. However, only 75.391 square kilometers of forest land remained during this time period Figure 11.

Drought and human activities are the main sources of the aforementioned forest change. For instance, the southern portion of the Awata River watershed, which is situated in the pastoralist area, experienced the greatest conversion of natural forest to shrubland due to drought. Additionally, anthropogenic operations were responsible for the conversion to mining, agricultural, wetland, and settlement areas. This is supported by Hamilton [47]. Major forest clearance believed to be associated with agriculture dates back to about 2000 BP in East Africa. However, in this study area, the primary factors of forest clearance were grazing land expansion, which in turn contributed to climate change (drought) and expanded shrubland in the area.

4. CONCLUSION

Using remote sensing techniques, this study examines changes in land cover and land use with a focus on the Aferara natural forest in the Awata River watershed. Satellite data from the Landsat series for the years 1985, 1994, 2004, and 2014, as well as Sentinel-2 data for 2023, were used to analyze changes, especially in the forest cover of the study area. The investigation was carried out using a random forest classifier within the Google Earth Engine platform environment, and additional analysis was conducted utilizing a variety of statistical and geospatial technology analysis tools. Forest land decreased significantly from 433.8 square kilometers in 1985 to 79 square kilometers in 2023, according to the results of land use and land cover change analysis. Concurrently, agricultural land, shrub land, settlement areas, and wetlands increased from 3.18, 120, 1.66, and 6.5 square kilometers in 1985 to 60.33, 339.1, 98.4, and 38.78 square kilometers in 2023, respectively. The rates of change in forest cover between 1985 & 1994, 1994 & 2004, 2004 & 2014, and 2014 & 2023 were 301.20, 207.51, 193.21, and 54.84 square kilometers annually. The overall annual rate of deforestation in the area was 67.58 square kilometers. The main causes of natural forest cover change in the basin include grazing, population growth, the extension of agricultural land, and various economic activities, which in turn lead to drought in the Awata River watershed.

Funding: This study received no specific financial support.
Institutional Review Board Statement: Not applicable.
Transparency: The author states that the manuscript is honest, truthful, and transparent, that no key aspects of the investigation have been omitted, and that any differences from the study as planned have been clarified. This study followed all writing ethics.
Competing Interests: The author declares that there are no conflicts of interests regarding the publication of this paper.

REFERENCES

[1] S. Jalayer, A. Sharifi, D. Abbasi-Moghadam, A. Tariq, and S. Qin, "Modeling and predicting land use land cover spatiotemporal changes: A case study in chalus watershed, Iran," *IEEE Journal of Selected Topics in Applied Earth Observations and Remote Sensing*, vol. 15, pp. 5496-5513, 2022. https://doi.org/10.1109/JSTARS.2022.3189528

[2] M. B. Moisa, I. N. Dejene, L. B. Hinkosa, and D. O. Gemeda, "Land use/land cover change analysis using geospatial techniques: A case of Geba watershed, western Ethiopia," *SN Applied Sciences*, vol. 4, no. 6, p. 187, 2022. https://doi.org/10.1007/s42452-022-05069-x

[3] G. Sisay, B. Gessesse, C. Fürst, M. Kassie, and B. Kebede, "Modeling of land use/land cover dynamics using artificial neural network and cellular automata Markov chain algorithms in Goang watershed, Ethiopia," *Heliyon*, vol. 9, no. 9, p. e20088, 2023. https://doi.org/10.1016/j.heliyon.2023.e20088

[4] T. Gashaw, T. Tulu, M. Argaw, and A. W. Worqlul, "Evaluation and prediction of land use/land cover changes in the Andassa watershed, Blue Nile Basin, Ethiopia," *Environmental Systems Research*, vol. 6, no. 1, p. 17, 2017. https://doi.org/10.1186/s40068-017-0094-5

[5] M. K. Leta, T. A. Demissie, and J. Tränckner, "Modeling and prediction of land use land cover change dynamics based on land change modeler (LCM) in nashe watershed, upper blue nile basin, Ethiopia," *Sustainability*, vol. 13, no. 7, p. 3740, 2021. https://doi.org/10.3390/su13073740

[6] H. Yunfeng and Y. Dong, "An automatic approach for land-change detection and land updates based on integrated NDVI timing analysis and the CVAPS method with GEE support," *ISPRS Journal of Photogrammetry and Remote Sensing*, vol. 146, pp. 347-359, 2018.

[7] M. F. Baig, M. R. U. Mustafa, I. Baig, H. B. Takaijudin, and M. T. Zeshan, "Assessment of land use land cover changes and future predictions using CA-ANN simulation for Selangor, Malaysia," *Water*, vol. 14, no. 3, p. 402, 2022. https://doi.org/10.3390/w14030402

[8] M. Mariye, L. Jianhua, M. Maryo, G. Tsegaye, and E. Aletaye, "Remote sensing and GIS-based study of land use/cover dynamics, driving factors, and implications in southern Ethiopia, with special reference to the Legabora watershed," *Heliyon*, vol. 10, no. 1, p. e23380, 2024. https://doi.org/10.1016/j.heliyon.2023.e23380

[9] M. Mishkin and J. A. N. Pacheco, "Rapid assessment remote sensing of forest cover change to inform forest management: Case of the Monarch reserve," *Ecological Indicators*, vol. 137, p. 108729, 2022. https://doi.org/10.1016/j.ecolind.2022.108729

[10] I. Potić *et al.*, "Improving forest detection using machine learning and remote sensing: A Case study in Southeastern Serbia," *Applied Sciences*, vol. 13, no. 14, p. 8289, 2023. https://doi.org/10.3390/app13148289

[11] B. Bera, S. Saha, and S. Bhattacharjee, "Forest cover dynamics (1998 to 2019) and prediction of deforestation probability using binary logistic regression (BLR) model of Silabati watershed, India," *Trees, Forests and People*, vol. 2, p. 100034, 2020. https://doi.org/10.1016/j.tfp.2020.100034

[12] B. Debebe, F. Senbeta, E. Teferi, D. Diriba, and D. Teketay, "Analysis of forest cover change and its drivers in biodiversity hotspot areas of the Semien Mountains National Park, northwest Ethiopia," *Sustainability*, vol. 15, no. 4, p. 3001, 2023. https://doi.org/10.3390/su15043001

[13] D. N. Pant, S. M. Groten, and P. Roy, "Forest vegetation/landuse change detection and impact assessment in part of western Himalaya," *International Archives of Photogrammetry and Remote Sensing*, vol. 33, no. B7/3; PART 7, pp. 1111-1118, 2000.

[14] M. A. Daniel and A. T. Salami, "Application of remote sensing and GIS inland use/land cover mapping and change detection in a part of south western Nigeria," *African Journal of Environmental Science and Technology*, vol. 1, no. 5, pp. 99-109, 2007.

[15] A. Thieme, E. Glennie, P. Oddo, S. McCartney, M. Ruid, and A. Anand, "Application of remote sensing for ex ante decision support and evaluating impact," *American Journal of Evaluation*, vol. 43, no. 1, pp. 26-45, 2022. https://doi.org/10.1177/1098214020962579

[16] N. Yahya, T. Bekele, O. Gardi, and J. Blaser, "Forest cover dynamics and its drivers of the Arba Gugu forest in the Eastern highlands of Ethiopia during 1986–2015," *Remote Sensing Applications: Society and Environment*, vol. 20, p. 100378, 2020. https://doi.org/10.1016/j.rsase.2020.100378

[17] A. Tariq *et al.*, "Modelling, mapping and monitoring of forest cover changes, using support vector machine, kernel logistic regression and naive bayes tree models with optical remote sensing data," *Heliyon*, vol. 9, no. 2, p. e13212, 2023. https://doi.org/10.1016/j.heliyon.2023.e13212

[18] F.-K. Gallon and J. Busch, "What drives deforestation and what stops it? A meta-analysis of spatially explicit econometric studies," *CGD Working Paper No. 361. Washington, DC: Center for Global Development*, 2014.

[19] I. M. D. Rosa, "Modelling land cover change in tropical rainforests," Doctoral Dissertation, Imperial College London, 2013.

[20] FAO, *The state of the world's forests: Forests, biodiversity and people*. Rome: National Strategy To Reduce Deforestation and Forest Degradation, 2020.

[21] OECD-FAO, *Draft OECD-FAO handbook on deforestation, forest degradation and due diligence in agricultural supply chains*. France: OECD-FAO, 2022.

[22] R. N. Masolele *et al*., "Mapping the diversity of land uses following deforestation across Africa," *Scientific Reports*, vol. 14, no. 1, p. 1681, 2024. https://doi.org/10.1038/s41598-024-52138-9

[23] J. A. Sayer and C. S. Harcourt, *The conservation Atlas of tropical forests Africa*. Cambridge: Digitized by the Internet Archive in 2010 with Funding from UNEP-WCMC, 2010.

[24] FAO, *Global forest resources assessment*. Rome: Food and Agricultural Organization of the United Nations, 2010.

[25] R. Matthias, "Change detection of natural high forests in Ethiopia using remote sensing and GIS techniques," *International Archives of Photogrammetry and Remote Sensing*, vol. 33, no. B7/3; PART 7, pp. 1253-1258, 2000.

[26] EFAP, *The challenge for development, draft final report*. Addis Ababa, Ethiopia: Ethiopia Forestry Action Program (EFAP), 1993.

[27] G. Rees, *Physical principles of remote sensing*. Cambridge, UK: Cambridge University Press, 2013.

[28] A. Scott, *Seeing the forest for the trees*. United Kingdom: Scott Logic Blog, 2023.

[29] R. Avtar, J. K. Thakur, A. K. Mishra, and P. Kumar, "Geospatial technique to study forest cover using ALOS/PALSAR data. In Geospatial techniques for managing environmental resources." Dordrecht: Springer Netherlands, 2012, pp. 139-151.

[30] M. L. Scott *et al*., "Mapping tree cover expansion in Montana, USA rangelands using high-resolution historical aerial imagery," *Remote Sensing in Ecology and Conservation*, vol. 10, no. 1, pp. 91-105, 2024. https://doi.org/10.1002/rse2.357

[31] M. H. Shahrokhnia and S. H. Ahmadi, "Remotely sensed spatial and temporal variations of vegetation indices subjected to rainfall amount and distribution properties. In H. R. Pourghasemi (Ed.), Spatial Modeling in GIS and R for Earth and Environmental Sciences." Amsterdam, Netherlands: Elsevier, 2019, pp. 21–53.

[32] K. P. Jessica, M. C. Porwal, P. S. Roy, and G. Sandhya, "Forest change detection in Kalarani round, Vadodara, Gujarat—a remote sensing and GIS approach," *Journal of the Indian Society of Remote Sensing*, vol. 29, no. 3, pp. 129-135, 2001. https://doi.org/10.1007/BF02989924

[33] A. Singh, "Review article digital change detection techniques using remotely-sensed data," *International Journal of Remote Sensing*, vol. 10, no. 6, pp. 989-1003, 1989. https://doi.org/10.1080/01431168908903939

[34] B. Aiazzi and F. Bovolo, "Change detection in multitemporal images through single- and multi-scale approaches. In Signal and Image Processing for Remote Sensing." Switzerland: Springer International Publishing, 2018, pp. 1–25.

[35] B. G. Tikuye, M. Rusnak, B. R. Manjunatha, and J. Jose, "Land use and land cover change detection using the random forest approach: The case of the Upper Blue Nile River Basin, Ethiopia," *Global Challenges*, vol. 7, no. 10, p. 2300155, 2023. https://doi.org/10.1002/gch2.202300155

[36] A. Barenblitt, L. Fatoyinbo, N. Thomas, A. Stovall, C. De Sousa, C. Nwobi, and L. Duncanson, "Invasion in the Niger Delta: Remote sensing of mangrove conversion to invasive Nypa fruticans from 2015 to 2020," *Remote Sensing in Ecology and Conservation*, vol. 10, no. 1, pp. 5-23, 2024. https://doi.org/10.1002/rse2.353

[37] L. Joongbin, K.-M. Kim, E.-H. Kim, and R. Jin, "Machine learning for tree species classification using sentinel-2 spectral information, crown texture, and environmental variables," *Remote Sensing*, vol. 12, no. 12, p. 2049, 2020. https://doi.org/10.3390/rs12122049

[38] B. Lucian, D. C. Ilieş, J. A. Wendt, I. Rus, K. Zhu, and L. D. Dávid, "Monitoring forest cover dynamics using orthophotos and satellite imagery," *Remote Sensing*, vol. 15, no. 12, p. 3168, 2023. https://doi.org/10.3390/rs15123168

[39] M. Paul, C. Fischer, H. Fuchs, and C. Kleinn, "Translating criteria of international forest definitions into remote sensing image analysis," *Remote Sensing of Environment*, vol. 149, pp. 252-262, 2014. https://doi.org/10.1016/j.rse.2014.03.033

[40] L. B. Szilárd, I. J. Holb, V. Oláh, P. Burai, and S. Szabó, "Deep learning-based training data augmentation combined with post-classification improves the classification accuracy for dominant and scattered invasive forest tree species," *Remote Sensing in Ecology and Conservation*, vol. 10, no. 2, pp. 203-219, 2024. https://doi.org/10.1002/rse2.365

[41] L. Wan-Ni, "Forest aboveground biomass monitoring in Southern Sweden using random forest model with sentinel-1, sentinel-2, and LiDAR data," Master's Thesis, Faculty of Engineering and Sustainable Development, Department of Computer and Geospatial Sciences, Sweden, 2023.

[42] A. Hua, "Application of CA-Markov model and land use/land cover changes in Malacca River watershed, Malaysia," *Applied Ecology & Environmental Research*, vol. 15, no. 4, pp. 605-622, 2017. https://doi.org/10.15666/aeer/1504_605622

[43] Y. Abyot, B. Gedif, S. Addisu, and F. Zewudu, "Forest cover change detection using remote sensing and GIS in Banja district, Amhara region, Ethiopia," *International Journal of Environmental Monitoring and Analysis*, vol. 2, no. 6, pp. 354-360, 2014. https://doi.org/10.11648/j.ijema.20140206.19

[44] O. S. Olokeogun, K. Iyiola, and O. F. Iyiola, "Application of remote sensing and GIS in land use/land cover mapping and change detection in Shasha forest reserve, Nigeria," *The International Archives of the Photogrammetry, Remote Sensing and Spatial Information Sciences*, vol. 40, pp. 613-616, 2014. https://doi.org/10.5194/isprsarchives-XL-8-613-2014

[45] IUCN, *Ethiopian national conservation strategy: Phase One.* Gland, Switzerland: IUCN, 1990.

[46] P. Pacheco *et al.*, *Deforestation fronts: Drivers and responses in a changing world.* Gland, Switzerland: WWF, 2021.

[47] A. C. Hamilton, "Environmental history of East Africa," in London, UK. Academic Press, 1982.